# Intensity Modulation of Medium-Energy, High Dose Rate Brachytherapy Sources

PHYSICS MAJOR QUALIFYING PROJECT

Matthew Jalbert
WORCESER POLYTECHNIC INSTITUTE | SUBMITTED TO DR. DAVID MEDICH

A Physics Major Qualifying Project Report
Submitted to the Faculty of
WORCESTER POLYTECHNIC INSTITUTE
in partial fulfillment of the requirements
for the Degree of Physics Bachelor of Science

by Matthew Jalbert

6 April 2020

Report Submitted to:

Associate Professor David Medich
Worcester Polytechnic Institute

# Acknowledgments

*I would like to thank the following people for their support of this project*

My advisor, **Dr. David Medich**, for his support, offering his expertise on Medical Physics and MCNP, and for being instrumental in my acquisition of MCNP.

PhD candidate, **Justine Dupere**, for offering her support and expertise on Brachytherapy and MCNP

# Table of Contents


ACKNOWLEDGEMENTS 3

TABLE OF CONTENTS 4

INTRODUCTION 5

BACKGROUND 6

- Nuclear and Medical Physics 6
- Radiation Oncology and Brachytherapy 6
- Monte Carlo N-Particle Transport Code 7

METHODS 9

- Create simulations of medium dose rate materials 9
- Identify differences between the output data from various materials and geometrical conditions 11

RESULTS 13

- Outputs 13
- Simulation Results 13

DISCUSSION 17

- Conclusions 18

REFERENCES 19

APPENDIX A: GAMMAS AND X-RAYS 20

- Iridium-192 20
- Ytterbium-169 21
- Selenium-75 23

APPENDIX B: MATERIAL CARDS 24

APPENDIX C: EXAMPLE CODE 25

# Introduction

Although Medical Physics is a relatively new field of study compared with other medical related fields, Medical Physics has rapidly evolved and is in high demand because it offers a different perspective on medical issues that cannot always be observed from a biological or chemical background. Most often, medical physics uses principles of nuclear and quantum physics to contribute to medical practices. One such example of this is Brachytherapy. Brachytherapy is the oncological practice of surgically implanting radioactive material into a patient in order to irradiate, and hopefully eliminate, a targeted tumor.

Brachytherapy is an effective way to irradiate tumorigenic cells while minimizing the irradiation of healthy tissue. This is important, as healthy tissue is also vulnerable to radiation. Medical physicists have devised methods for the safe use of medical radiation in brachytherapy. One option to reduce damage to healthy tissue is to choose a lower energy material, however this will also reduce the dose absorbed by the tumor cells per unit time. Another more precise method is to use shielding to protect healthy tissue. Perhaps the largest benefit of shielding is that the geometry can be adjusted accordingly to "aim" the radiation at a tumor while shielding healthy tissue. This can be done by deliberately shaping the shielding to leave part of the radioactive material (or pellet) exposed, then aiming the exposed section at tumor cells. In addition to this, the thickness of the shielding can also be changed. These practices are known as intensity modulated brachytherapy.

The purpose of this project is to evaluate the viability of Ytterbium-169 and Selenium-75 as intensity modulated brachytherapy sources. As alluded to previously, some radioactive materials may be more fit for brachytherapy than others. One of the more common sources used in the practice is Iridium-192. The medical community always proceeds on the side of caution, so viable sources that are lower energy are well sought out. Yb169 and Se75 are two such sources. It is hypothesized that these medium-energy high dose rate sources are easier to energy modulate than the high dose rate source Ir192. Therefore, this project will be measuring how effective gold shielding is with each material. The results of this project will hopefully indicate that it would be beneficial to conduct further research on Yb169 and Se75 and the effects of brachytherapy intensity modulation.

# Background

## Nuclear and Health Physics

Brachytherapy sources emit electromagnetic radiation in the process of nuclear transformation and radioactive decay. The United States Nuclear Regulatory Commission (2019) defines radioactive decay as "The spontaneous transformation of one radioisotope into one or more different isotopes (known as "decay products" or "daughter products"), accompanied by a decrease in radioactivity (compared to the parent material) …" Isotopes, such as Ir192, have unstable nuclei; due to nature's 'desire' to be in a stable state of equilibrium, isotopes go about various methods of achieving this. In radioactive isotopes, nuclear bonds are broken and in turn energy in the form of gamma rays and x-rays can be emitted. It is impossible to predict exactly when a single nucleus will go through this transformation, but a rate of decay can be determined with large quantities of nuclei.

Incident photons are emitted towards nearby materials where another interaction may occur. If a photon interacts with an atom, it may bounce off the atom (scatter) or have its energy fully absorbed by the nucleus. The chances these interactions are dependent on the material; some materials (specifically high-Z materials) are better at scattering photons than others. This concept is used in everyday life, from the use of lead to protect patients and doctors from x-rays, to the use of gold to shield satellite instruments from solar radiation. Furthermore, blocking harmful radiation is also a fundamental property of the Earth's atmosphere. These reactions are impossible to individually predict but it is possible to determine, the ratio of photons that experience a collision to the photons that do not. This value is determined with the density and thickness of the material – alongside the attenuation coefficient, which varies with the material and the photon.

It is known that electromagnetic radiation can be hazardous to humans and living things since radiation absorbed by cells can damage these cells – thus, its connection to cancer; causing damage to cells comes with an increased chance of tumorigenesis. Generally, small amounts of radiation exposure are harmless, but larger amounts can lead to radiation sickness or even death. The amount of absorbed radiation is called the absorbed dose, measured by energy absorbed per unit mass. The SI unit of dose is Gray (Gy) which converts to $6.24E12(MeV)(kg)^{-1}$ (Turner, 1995).

## Radiation Oncology/Brachytherapy

Because tumorigenic cells undergo mitosis more rapidly than their healthy counterparts, cancer cells are significantly more sensitive to the damaging effects of radiation than their normal cell counterparts. Because of this, radiation is used to treat cancer. This practice, called radiation

therapy, is defined by the National Cancer Institute (2019) as “a cancer treatment that uses high doses of radiation to kill cancer cells and shrink tumors.” Radiation therapy was developed alongside the development of medical imaging practices, namely x-ray imaging. The first published x-ray image was taken in 1895 by Wilhelm Conrad Roentgen, a year later x-rays were used as treatment for breast cancer (Skowronek, 2017). Soon thereafter, Pierre Curie suggested to insert radioactive material into a tumor in order to eliminate it, this practice was later used and is now called brachytherapy (Skowronek, 2017). Over the next century, physicists expanded the understanding of radiation and its effects of human physiology and anatomy. This better understanding led to the safer and more effective radiation therapies implemented today.

*Figure 1. Size comparison between brachytherapy seeds and a US cent. (Wikimedia.org, 2018)*

Radon, radium and cobalt isotopes were some of the first used brachytherapy source and were prevalent from the 1930s to the 1950s when Iridium-192 rose to become the most common source (Skowronek, 2017). Small quantitates of these materials are shaped into small cylinders and cover with gold shielding, as seen in figure 1. Gold has always been the standard shielding for brachytherapy, the metal is an effective shield and more importantly is a biocompatible material, meaning it will not interfere with human physiology. As nuclear technology has improved over the past century, clinics have gained access to a greater variety of radionuclides, including sources with lower energies than the current gold standard, Ir192. Yet if a brachytherapy source emits photons with too low an energy, then those photons are absorbed quickly and therefore can’t be used to irradiate thick tumors. Alternatively, medium energy sources may be the best balance since they can uniformly irradiate thick tumors yet can be easily shielded with high-Z materials such as lead, gold, or platinum. Among these medium energy sources are Ytterbium-169 and Selenium-75.

Ir192 currently is the gold standard for brachytherapy because it has many mid-energy photons and lower yield high energy photons. Additionally, the source is very cost effective to produce. However, Ir192 is still a high-energy source requires large amounts of lead shielding to be considered safe. In contrast, Yb169 and Se75 have significantly lower dose rates, allowing for the use of even less shielding.

## Monte Carlo N-Particle Transport Code

The Monte Carlo n-Particle Code 6 (MCNP6) was used to simulate the three chosen brachytherapy sources. Monte Carlo simulations use randomness and are probabilistic making MCNP6 well suited to simulate the probabilistic nature of quantum and nuclear mechanics.

MCNP6 was developed by Los Alamos Laboratory in 2018. VisEd, MCNP6's visual editor software, is useful for visualizing the geometry of the physical set up of materials used in a specific code. In addition to this it can be used to show how MCNP6 would simulate particle interactions. In the case of figure 2, VisEd demonstrates how when commanded to simulate 1,000 particle interactions, MCNP will simulate each particle interaction independently, in a random location – similar to how an isotope might decay.

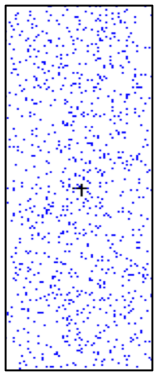

*Figure 2. VisEd demonstrates how MCNP is able to generate particle interactions randomly*

# Methods

The goal of this project was to measure the degree that Yb169, Se75 and Ir192 can have their dosimetric output modulated with gold shielding in a brachytherapy setting. This improved understanding may indicate that further research on medium dose rate brachytherapy sources would be constructive in improving oncological practices. To achieve this goal the following objectives were completed:

1. Create simulations of medium dose rate materials.
2. Identify differences between the output data from various materials and geometrical conditions

## Create simulations of medium dose rate materials

Yb169 and Se75 were chosen as medium does rate sources and Ir192, a high-energy source, would be simulated for the purposes of comparison. The code would start out as a simple point source in a volume of water. In this step, surfaces defined from a spherical cell was made into a volume of $1m^3$ of water with the elemental composition defined using the MCNP materials card (Appendix B). For the purpose of being time efficient the number of particles simulated (nps) of these preliminary codes was kept at 100000 which correlating to a relative error lower than 5%. From there, the code was built up step by step, after each step or group of steps, the code was executed and its outputs were verified by Dr. David Medich. Next, cell and surface cards were added to the code, changing the point source to a cylindrical source, as shown in figure 3.

```
c      ---CELL CARDS---
504  2  -6.00  (-116 +118 -119) imp:p,e=1
c    water phantom
561  1  -0.998 (#504 -400)      imp:p,e=1
c    end of simulated world
999  0         (+400)           imp:p,e=0

c     ---SURFACE CARDS---
c    Pellet. (cylinder)
116  CZ  0.04 $ Cylinder radius
118  PZ -0.11 $ Bottom Plane
119  PZ  0.11 $ Top Plane
c    end of the world
400  SO 133.5
```

*Figure 3. Code describing the geometry of brachytherapy source.*

The source definition card (sdef) was then written to correctly represent the correct volume of where photons would be produced, seen in figure 4. Par=2 indicates to MCNP that the source is emitting photons. Pos=d1 indicates that the reference point for the system is defined by si1 and sp1. These commands state that the reference point is located at the origin and the particles are emitted uniformly throughout the area. Rad=d2 indicates the distance between the reference

```
c  Source Definitions
sdef   par=2 pos=d1 rad=d2 axs=0 0 1 ext=d3 erg=d4
si1    L  0 0 0
si1    1.0000
si2    0.000  0.04
sp2    -21  1
si3    -.11 .11
sp3    0    1
```

*Figure 4. Code describing the location and details of photon production.*

point and the source using si2 and sp2 commands. Here, the source position ranges from the reference point to .04cm and also results in an equal sampling length. Ext=d3 works similarly, using si3 and sp3, the source is defined as ranging from -0.11 to 0.11 on the z axis. The z axis was determined by the command AXS=0 0 1. Finally, the erg=d4 describes the gamma and x-ray energies and frequencies of the specific source material used (Appendix A). These values were found from an online collection of data on radioactive isotopes (Chu, 1999).

Next a mesh tally was developed to measure the dose absorbed in individual areas, seen in figure 5. This was integral for measuring how dose changed as a function of distance from the source. Later on, it would also become integral for showing the effectiveness of shielding in lowering absorbed dose. The mesh tally changed throughout the building process of the code, initially only measuring doses delivered to different distances. Later measuring dosage to different angles oriented about the z axis.

```
*FMESH04:p  Geom = cyl  Origin = 0 0 -0.5
            AXS 0 0 1           VEC +1 0 0
            IMESH = 1 10        IINTS = 1 9
            JMESH = 1             JINTS = 1
            KMESH = 1           KINTS = 360
            OUT = col
FM04  2E10
```

*Figure 5. Code describing the specifics of how and where energy absorption is measured.*

The first line of this code segment denotes that this is a tally counting photon interactions in locations described by a cylindrical coordinate system with a reference point and the vector <0,0,-0.5>cm. The second line denotes the z axis as the parallel to the cylindrical tally positions and the positive x axis as the starting point of where the angles will be measured from. The IMESH and IINTS commands correspond to the radial distance from the origin on the xy plane. IMESH = 1 10 indicates that tallies will be taken within two ranges, 0 to 1 and 0 to 10. The IINTS inputs are respective to the IMESH inputs, IINTS = 1 9, indicates that there will be one tally measurement between 0cm and 1cm and another nine tally measurements between 0cm and 10cm. This resulted in measurements at 0.5, 1.5, 2.5, 3.5… and 9.5cm. The tally measurements are evenly spaced out with the set ranges. JMESH and JINTS correspond to the tallies along the z axis. As one can deduce there is one tally measurement between 0cm and 1cm at 0.5cm, however because the reference point is located -0.5, the actually tally measurements are taken exactly on the xy plane. Lastly, KMESH and KINTS correspond to the angle from the positive x axis, which is in units of revolutions. Here there are 360 measurements taken within the revolution. The FM04 2E10 command is a multiplier to make yield more realistic results in a brachytherapy context.

The final major alteration to the code was creating the cell, surface and material cards for the gold shielding, seen in figure 6. It was decided to obtain simulation data with shielding open 10, 30, 60, 90, 120, 150 and 170 degrees. Additionally, the simulation would be run with the shield

thicknesses of, 100, 200 and 300 microns. It was crucial for the code to be easy to adjust to simulate different shield openings and different thicknesses. Every combination of material, thickness and opening angle corresponded to a specific text file designed to be executed through MCNP6.2.

```
Shield siding
121 CZ  0.04
122 CZ  0.04 + T
c
c  Shield Bottom Cap
123 PZ -0.11
124 PZ -0.12
c
c  Shield Top Cap
125 PZ  0.11
126 PZ  0.12
c
c  Dividing planes to vary shield
opening
140 P  N  1  0  0.0001
150 P  N -1  0 -0.0001
```

*Figure 6. Code describing the geometry of shielding, with varying factors T (thickness) and N (angle of shield opening).*

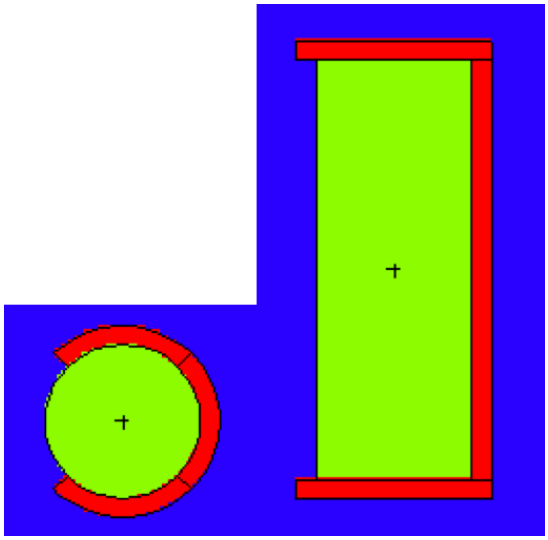

*Figure 7. VisEd depictions of a top (left) and side (right) view of shielded brachytherapy source.*

Above are the surface designations for the shielding. Surfaces 121-126 describe the top, bottom and siding of the shielding. To change the thickness of the siding the value T can be changed to a desired thickness which here is the difference between the value of surface 122 and the value of surface 121. Since the tallies measure the dosage at z=0, the thickness of the top and bottom shielding results in little to no difference on the dose absorbed. With the help of VisEd, it was determined that the angle of opening could be created by using two intersecting planes. The angle between these two planes would serve as the angle of opening. In the code, N serves to change the angle of opening. N is calculated as

$$N = \tan\left(\frac{\theta}{2}\right)$$

Where θ is the desired angle of shield opening. For example, to create an opening of 90°, N would be 1. A final version of the code can be found in Appendix C.

## Identify differences between the output data from various materials and geometrical conditions

The resulting mesh output files of the code were copied and pasted in a spreadsheet. From there the results would be organized and separated by distance from the tally reference point. A graph was created for each of these data sets. Each of these graphs plot the dose absorbed as

a function of angle from the x axis at a fixed distance. This will visually display the difference of how the geometry of gold shielding effects dose distribution to surrounding tissue. On the same note, the percent differences between the average dose absorbed by the unshielded and that shielded areas were also calculated. Below is the equation used to calculate this percent difference.

$$\triangle = 100 \times (1 - 100 \frac{avg_{shielded}}{avg_{exposed}})$$

# Results

## Outputs

Simulating 100,000 resulted in run times under ten seconds. In turn, the relative error yielded from these codes was also consistently over 1%, occasionally being as high as 4%. In turn, data gained from these codes was not usable, but was still useful in ensuring that the code was operating correctly. Despite the high relative error, it was still possible to discern that the shielding geometry was correctly described in the code.

The NPS of the final codes was raised to 50,000,000 (increased by a factor of 50). This resulted in a great decrease in relative error. The average relative error from the all the simulations was 0.798%. Relative error varied across materials; Yb169 had a relative error of 1.004%, Ir192 had 0.700%, and Se75 had 0.695%. This precision required a run time around 30 minutes for each of the individual codes.

## Simulation Results

As predicted, the Ir192 source delivered the most dose to the surrounding material, distantly followed by the Se75 and Yb169 sources.

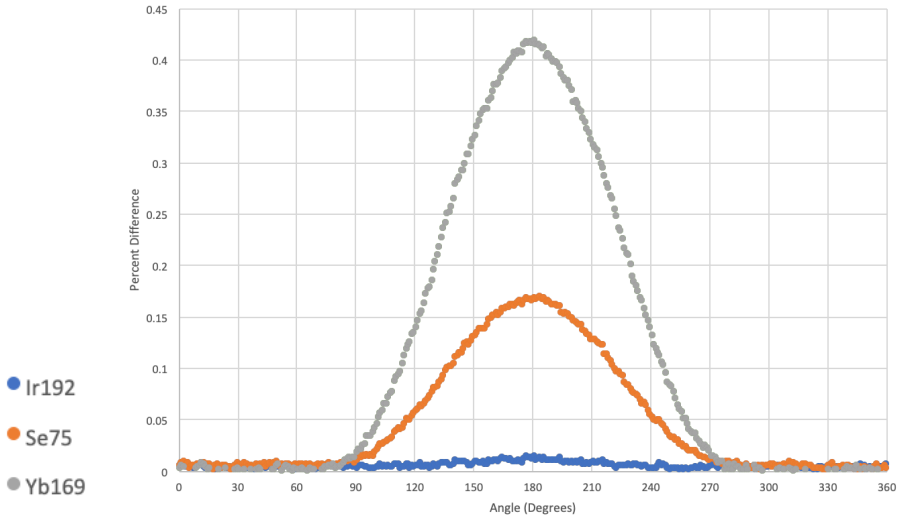


*Figure 8. Graph depicting the difference between Ir192 (blue), Se75 (orange) and Yb169 (grey), with 100micron shielding open 90°.*

Figure 8 shows the simulated results, 0.5cm from the source, when the shielding used is 100microns thick, open to a 90° angle. The graph represents the data from each material's

simulation normalized to the minimum calculated absorbed dose in each data set. In other words, the graph compares the effectiveness of 100microns of shielding against the three source materials. There is over a 40% difference between the lowest and highest absorbed dose of Yb169 (in grey) radiation. Meanwhile the percent difference between Ir192's (in blue) lowest and highest data points is less that 2%.

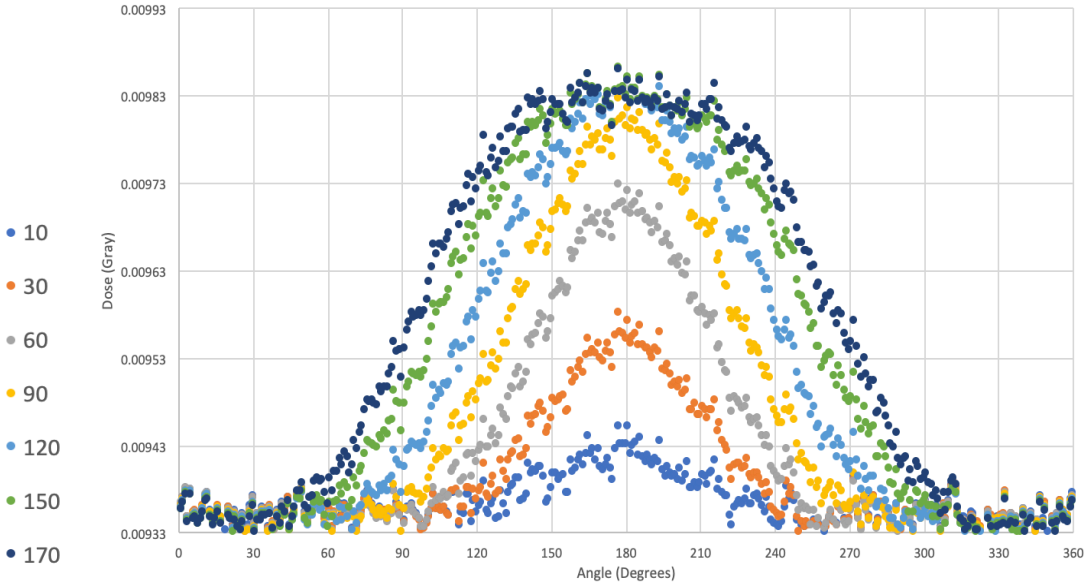


*Figure 9. Graph of Ir192 source, with 100micron shielding open to various angles.*

Figure 9 depicts how the angle of shield opening affects the dose absorbed by the surrounding area. Specifically, this graph used data from a simulated Ir192 source with 100micron gold shielding. Note that the y axis which has been shifted approximately to the shielded dose rate. The shield opening effects the total absorbed dose in the unshielded region, this effect lessens as the shield opens wider. As portrayed in the graph, there is relatively little difference in the max dose observed when the shielding was open more than 90°. Contrastingly, the difference the max dose observed from shielding open 10° and 30° is relatively large. As one might predict, the curve of each group of measurements becomes wider as the shield is open to a wider angle, meaning more area is being irradiated. It should also be noted that there is a difference in the doses absorbed by the unexposed areas between different shield openings.

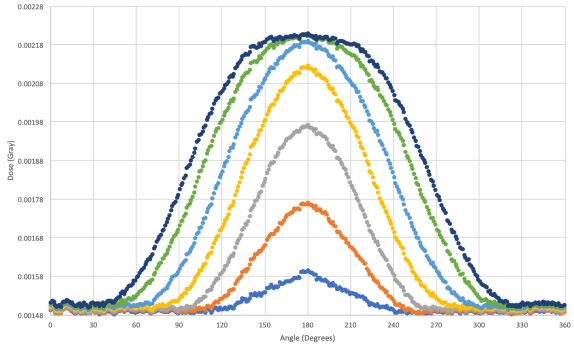


*Figure 10. Graph of Yb169 source, with 100micron shielding open to various angles.*

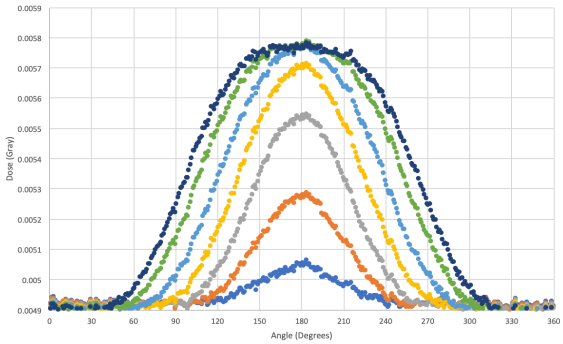


*Figure 11. Graph of Se75 source, with 100micron shielding open to various angles.*

Similar to figure 9, figures 10 and 11 depict the data from the simulated medium dose rate sources (Yb169 and Se75 respectively) with 100micron shielding open to various. What is learned from these graphs is that even though all these materials have different dose rates, they all behave similarly relative to their respective dose rates under these conditions. This is made evident from the fact that the shape of each curve representing data corresponding to a certain shield opening, is roughly the same shape for all these source materials.

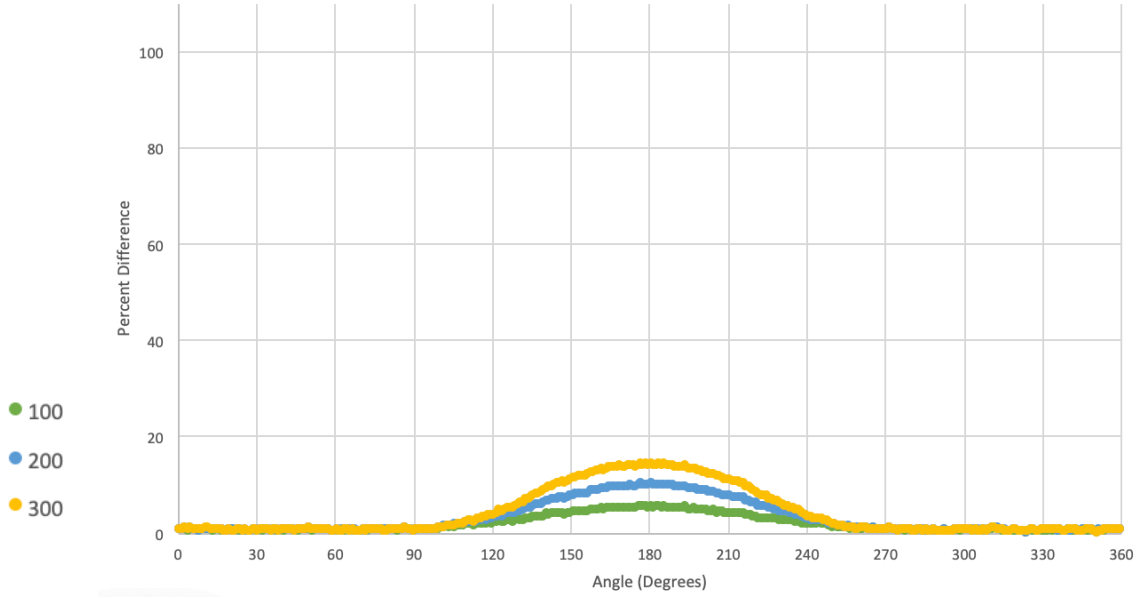


*Figure 12. Graph of Ir192 source, with various shield thicknesses, open 90°.*

The above graph depicts Ir192 under several conditions where the shielding is open to a 90° angle. The green, blue and yellow data points represent data from a simulation using 100, 200 and 300micron shielding respectively. Like the figure 9, the data sets have been normalized, in order to simplify comparing these measurements. 100microns of shielding was only able to block approximately 3% of the radiation outputted by the Ir192 source. In turn, 200microns

blocked approximately 7% of radiation and 300microns blocked approximately 9%. The numerical values corresponding to these measurements will be briefly discussed in the subsequent section.

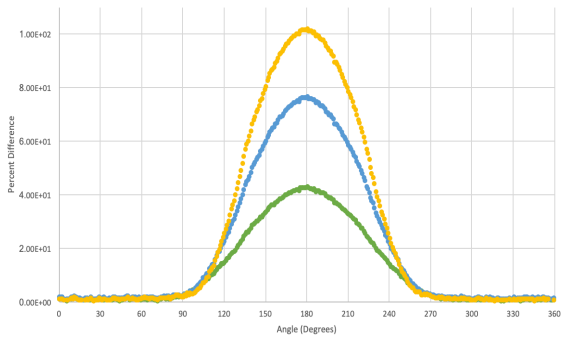


*Figure 13. Graph of Yb196 source, with various shield thicknesses, open 90°.*

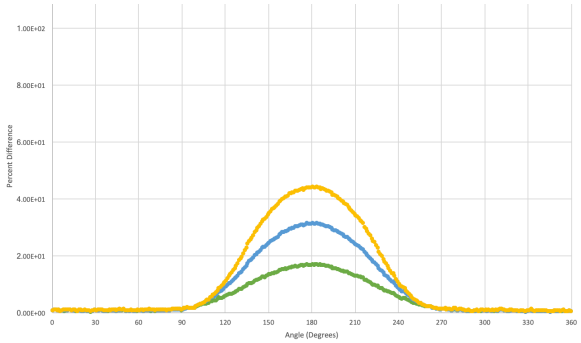


*Figure 14. Graph of Se75 source, with various shield thicknesses, open 90°.*

Similar to the previous graph, the two above graphs depict the normalized data from the simulated medium dose rate sources (Yb169 and Se75 respectively) with shielding open to a 90° angle varying in shield thickness. The gold shielding proved to be more effective against the medium dose rate sources, especially the weaker Yb169 source. 100microns of shielding blocked 23% of Yb169 radiation. Subsequently, 200microns blocked approximately 35% of radiation and 300microns blocked approximately 42%. In as for Se75 radiation, 100 microns of shielding blocked 11%, 200microns blocked 19% and 300microns blocked 24%.

These percent differences should not be confused with the percent differences between maximums and minimums discussed earlier. These percentage differences are calculated from the average values from the shielded area, using the average values from the unshielded area as a base. Below are tables summarizing these findings relatively and quantitatively.

| | **SHIELDING THICKNESS (MICRONS)** | | |
|---|---|---|---|
| **PERCENTAGES** | **100** | **200** | **300** |
| IR192 | 3% | 7% | 9% |
| YB169 | 23% | 32% | 45% |
| SE75 | 11% | 19% | 24% |

| **VALUES (GY)** | **100** | **200** | **300** |
|---|---|---|---|
| IR192 | 3.32E-4±5.11E-7 | 6.29E-04±9.94E-7 | 8.98E-04±1.44E-6 |
| YB169 | 4.64E-4 ±1.14E-6 | 6.76E-04±1.87E-6 | 8.01E-04±2.37E-6 |
| SE75 | 5.92E-4±1.04E-6 | 1.01E-03±1.67E-6 | 1.32E-03±2.44E-6 |

# Discussion

Due to their lower energy, Yb169 and Se75 sources were more effectively shielded using 100-300microns of gold than the Ir192 source. Ir192's high energy comes with this drawback; the various thicknesses in gold shielding were barely able to block any Ir192 radiation. 300microns of shielding wasn't enough to block 10% of Ir192 radiation. Furthermore, 100microns of shielding only blocked 3% of Ir192 radiation – at which point, it likely is not cost effective to use shielding at all. Unless a treatment plan is willing to shielding with thicknesses greater than a millimeter, Ir192 will irradiate any surrounding healthy tissue just as much as it irradiates the tumor. Not only is this strategy not cost effective, it also defeats the point of using a Ir192 source in situations which call for small shield openings. As seen in figure 15 depicting data from Ir192, the thickness of the shielding has a hindering effect on dose absorbed in unshielded areas. Increasing shield thickness from 100 to 300microns caused a 5% decrease in dose in unshielded areas. This figure seems insignificant until one remembers that 300microns of shielding only blocked 9% of radiation in shielded areas. In all, using shielding for Ir192 pellets is not very effective.

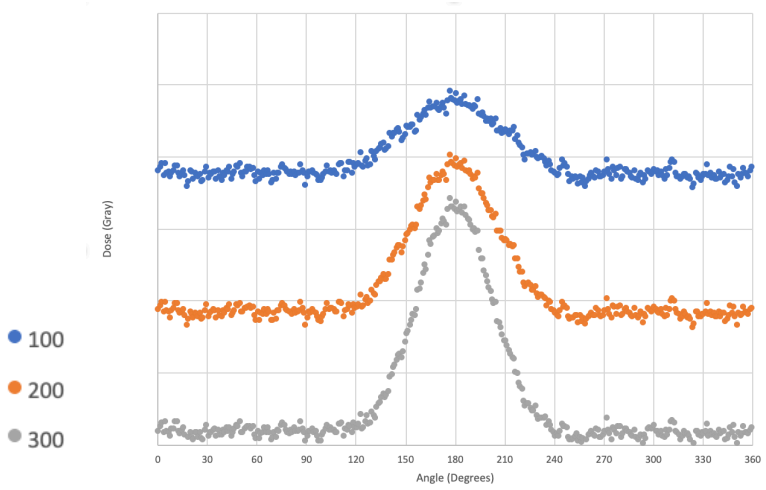


*Figure 15. Graph of Ir192 source, with various shield thicknesses, open 30°.*

In defense of Ir192, it is relatively inexpensive, and has a long half-life of 74.2 days (Krane, 1988), making it very usable. It's high dose rate, although not easily modulated, is advantageous when working in situations where healthy tissue is less at risk. However, gold shielding proved to be much more effective against these medium dose rate sources.
The dose rates of Yb169 and Se75 were much easier to modulate. 300microns of shielding was able to block 45% and 24% of Yb169 and Se75 radiation respectively. 100microns of shielding, blocked 23% of Yb169 radiation. The percentage associated with the Se75 source again lagged

behind, 100microns of shielding only blocked 11% of Se75 radiation, although quantitatively, shielding (of all thicknesses) was most effective against Se75 radiation. Quantitative results must be taken with a grain of salt, as radiation activities in these simulations were not designed to reflect those one can expect in a clinical setting. It may be worth refining these simulations to more closely mimic a brachytherapy system in future research. Research like this might include coding for source casings and data cards specific to organs than may be more or less vulnerable to radiation

Shielding against Yb169 is, on average, 5.3 times more effective than shielding against Ir192; and shielding against Se75 is, on average, 2.8 times more effective than shielding against Ir192. These figures provide a strong case for Se75 and especially for Yb169. Being able to irradiate tumorigenic tissue nearly twice as much as healthy tissue is extremely advantageous. Yb169 brachytherapy may be effective against smaller tumors that are located near organs sensitive to radiation. Se75 radiation is more difficult to modulate than Yb169 radiation but, is also about 3 times more powerful. Se75 is a decent middle ground between Yb169 and Ir192.

## Conclusions

Gold shielding is an effective intensity modulator for use in Ytterbium-169 and Selenium-75 brachytherapy. Selective shield openings allow for a substantial amount of radiation to be absorbed by tumor cells while limiting damage to healthy cells. Furthermore, increasing the thickness of the shielding grants even more protection to healthy tissue. Although these medium dose rate sources cannot hope to irradiate tumors at the rate of Iridium-192, the gold shielding is much more effective against these medium dose rate materials. Therefore, Yb169 and Se75 prove to be promising subjects for further research on intensity modulated brachytherapy.

# References


Brachytherapy (Internal radiation therapy). (2019, May 1). Retrieved from https://www.radiologyinfo.org/en/info.cfm?pg=brachy

Chu, S., Ekström, L., & Firestone, R. (1999, February). 75Se. Retrieved from http://nucleardata.nuclear.lu.se/toi/nuclide.asp?iZA=340075

Chu, S., Ekström, L., & Firestone, R. (1999, February). 169Yb. Retrieved from http://nucleardata.nuclear.lu.se/toi/nuclide.asp?iZA=700169

Chu, S., Ekström, L., & Firestone, R. (1999, February). 192Ir. Retrieved from http://nucleardata.nuclear.lu.se/toi/nuclide.asp?iZA=770192

Decay, radioactive. (2019). Retrieved from https://www.nrc.gov/reading-rm/basic-ref/glossary/decay-radioactive.html

Gianfaldoni, S., Gianfaldoni, R., Wollina, U., Lotti, J., Tchernev, G., & Lotti, T. (2017). An Overview on Radiotherapy: From Its History to Its Current Applications in Dermatology. Open Access Macedonian Journal of Medical Sciences, 5(4), 521-525. doi:10.3889/oamjms.2017.122

Krane, K. S., & Halliday, D. (1988). Introductory nuclear physics. Danvers, MA: Wiley & Sons.

Mayo Clinic Staff. (2018, March 28). Brachytherapy. Retrieved from https://www.mayoclinic.org/tests-procedures/brachytherapy/about/pac-20385159

Radiation Therapy for Cancer. (2019, January 8). Retrieved from https://www.cancer.gov/about-cancer/treatment/types/radiation-therapy

Radioactive Seeds. (2012, August 23). Retrieved from https://commons.wikimedia.org/wiki/File:Radioactive_Seeds_(7845754328).jpg

Skowronek, J. (2017). Current status of brachytherapy in cancer treatment – short overview. Journal of Contemporary Brachytherapy, 9(6), 581-589. doi:10.5114/jcb.2017.72607

Turner, J. E. (1995). Atoms, radiation, and radiation protection (2nd ed.). New York, NY: John Wiley & Sons.

Zaorsky, N., Davis, B., Nguyen, P., Showalter, T., Hoskin, P., Yoshioka, Y., . . . Horwitz, E. (2017). The evolution of brachytherapy for prostate cancer [Abstract]. Nature Reviews Urology, 14, 415-439. doi:https://doi.org/10.1038/nrurol.2017.76

# Appendix A: Gammas and X-rays

## Iridium192

| Energy (MeV) | Frequency |
|---|---|
| 0.110093 | 0.000126 |
| 0.13634348 | 0.00183 |
| 0.17698 | 0.000043 |
| 0.2013112 | 0.00472 |
| 0.20579549 | 0.003300 |
| 0.2147 | 0.000026 |
| 0.2147 | 0.000026 |
| 0.28004 | 0.00023 |
| 0.2832668 | 0.00262 |
| 0.29595827 | 0.2867 |
| 0.30845692 | 0.3000 |
| 0.3148 | 0.0007 |
| 0.3148 | 0.0007 |
| 0.31650791 | 0.8281 |
| 0.329312 | 0.000185 |
| 0.3744852 | 0.00721 |
| 0.4154 | 0.00009 |
| 0.4154 | 0.00009 |
| 0.4164714 | 0.00664 |
| 0.420532 | 0.000737 |
| 0.46807152 | 0.4783 |
| 0.4845780 | 0.03184 |
| 0.48530 | 0.000022 |
| 0.489039 | 0.00443 |
| 0.5885845 | 0.04515 |
| 0.59337 | 0.000426 |
| 0.59935 | 0.000039 |
| 0.60441464 | 0.0823 |
| 0.61246564 | 0.05309 |
| 0.70398 | 0.000053 |
| 0.739 | 0.0000050 |
| 0.739 | 0.0000051 |
| 0.7658 | 0.0000149 |

| | |
|---|---|
| 0.8845418 | 0.002923 |
| 1.06148 | 0.000528 |
| 1.0897 | 0.0000108 |
| 1.3783 | 0.0000124 |
| 0.060903 | 0.0000106 |
| 0.06148 | 0.0120 |
| 0.06300 | 0.0207 |
| 0.06414 | 0.0000286 |
| 0.06122 | 0.0265 |
| 0.06831 | 0.0453 |
| 0.71079 | 0.00239 |
| 0.71414 | 0.00460 |
| 0.71875 | 0.000113 |
| 0.073363 | 0.00162 |
| 0.073590 | 0.000188 |
| 0.075368 | 0.00533 |
| 0.075749 | 0.01029 |
| 0.076233 | 0.000265 |
| 0.077831 | 0.00365 |
| 0.078073 | 0.000478 |

## Ytterbium169

| **Energy (MeV)** | **Frequency** |
|---|---|
| 0.00841031 | 0.00333114 |
| 0.020752 | 0.0019014 |
| 0.06312077 | 0.4426 |
| 0.072028 | 0.000036 |
| 0.085093 | 0.000029 |
| 0.09361514 | 0.02614 |
| 0.098005 | 0.000018 |
| 0.101405 | 0.00007 |
| 0.1051910 | 0.0000268 |
| 0.10977987 | 0.174718 |
| 0.113976 | 0.00009 |
| 0.117377 | 0.00039721 |
| 0.11819018 | 0.0186918 |
| 0.13052368 | 0.11319 |

| | |
|---|---|
| 0.156725 | 0.01003 |
| 0.17721402 | 0.221618 |
| 0.19315 | 0.007410 |
| 0.19795788 | 0.3583 |
| 0.20599 | 0.00004084 |
| 0.213936 | 0.000029021 |
| 0.2263 | 0.000002518 |
| 0.22871 | 0.0000039 |
| 0.240332 | 0.00113814 |
| 0.26107857 | 0.0171511 |
| 0.291190 | 0.000043014 |
| 0.29454 | 0.000009725 |
| 0.3016 | 0.000047 |
| 0.30773757 | 0.10057 |
| 0.333965 | 0.000017914 |
| 0.336620 | 0.000090914 |
| 0.35674 | 0.000001406 |
| 0.370856 | 0.0000726 |
| 0.379286 | 0.000012218 |
| 0.386673 | 0.0000034011 |
| 0.45262 | 0.000000164 |
| 0.46472 | 0.00000003621 |
| 0.465657 | 0.00000189721 |
| 0.466562 | 0.00000019321 |
| 0.474973 | 0.000001934 |
| 0.494360 | 0.0000148625 |
| 0.50035 | 0.0000000888 |
| 0.5078 | 0.0000000158 |
| 0.515104 | 0.00004147 |
| 0.528572 | 0.000001757 |
| 0.54616 | 0.0000000154 |
| 0.562413 | 0.000001184 |
| 0.57089 | 0.0000012511 |
| 0.579854 | 0.00001923 |
| 0.600607 | 0.0000113121 |
| 0.624885 | 0.000049018 |
| 0.63332 | 0.0000000695 |
| 0.642877 | 0.00000075918 |

| | |
|---|---|
| 0.663603 | 0.000001896 |
| 0.69346 | 0.0000000874 |
| 0.710358 | 0.00000031121 |
| 0.73942 | 0.000000018321 |
| 0.76024 | 0.000000008221 |
| 0.773390 | 0.000002074 |
| 0.78164 | 0.000000030125 |
| 0.050742 | 0.940 |
| 0.057300 | 0.0993 |
| 0.057505 | 0.0192 |
| 0.057898 | 0.00379 |
| 0.059028 | 0.0647 |
| 0.059210 | 0.0172 |

## Selenium75

| **Energy (MeV)** | **Frequency** |
|---|---|
| 0.01488461 | 0.0000126 |
| 0.024381514 | 0.00027012 |
| 0.06605188 | 0.0111211 |
| 0.080936415 | 0.00007724 |
| 0.09673401 | 0.0342019 |
| 0.121115511 | 0.1723 |
| 0.13600016 | 0.5837 |
| 0.198606012 | 0.01484 |
| 0.24933 | 0.0000009424 |
| 0.26465769 | 0.589018 |
| 0.27954221 | 0.24995 |
| 0.30392361 | 0.013165 |
| 0.3736124 | 0.000024724 |
| 0.40065728 | 0.11477 |
| 0.41913 | 0.0001183 |
| 0.46864 | 0.00000348 |
| 0.5420217 | 0.0000013024 |
| 0.5569017 | 0.0000003512 |
| 0.5722224 | 0.0003564 |
| 0.61783 | 0.000044412 |
| 0.8215617 | 0.000001371 |

# Appendix B: Material Cards

## Iridium192

m3 77000.04p -1.0000

## Ytterbium169

m3 70000.04p  0.4000  8000.04p  0.6000

## Selenium75

m3 34000.04p  0.2000  8000.04p  0.8000

# Appendix C: Example Code

```
Cylindrical Source
c  Cylinder parallel to z axis
c  Done with cylindrical mesh tallies in 1mm increments
c  Water phantom
c
c  Written by Matt Jalbert Dec. 4, 2019
c  Code adapted from code:
c  IA10.txt by John Munro, 2009
c  IA10_water.txt edited by Norbert Hugger, 2018
c
c  ---CELL CARDS---
c  Brachytherapy source
504  3  -06.00  (-116 +118 -119)  imp:p,e=1
c
c  Shield Caps
517  4  -19.32  (-122  125 -129)  imp:p,e=1
518  4  -19.32  ( 124 -123 -122)  imp:p,e=1
c
c  Shield Siding
519  4  -19.32  ( 123 -125  140  150  121 -122)  imp:p,e=1
520  4  -19.32  ( 123 -125  140 -150  121 -122)  imp:p,e=1
521  4  -19.32  ( 123 -125 -140  150  121 -122)  imp:p,e=1
c
c  1m^3 of about water
561  1  -0.998  (#504 #519 #517 #518 -400 #520 #521)  imp:p,e=1
c
c  End of World
999  0  (+400)  imp:p,e=0
c

c  ——SURFACE CARDS——
c  Source
116 CZ  0.04
118 PZ -0.11
119 PZ  0.11
c
c  Shield siding
121 CZ  0.04
122 CZ  0.04+T
c
c  Shield Bottom Cap
```

```
123 PZ -0.11
124 PZ -0.12
c
c  Shield Top Cap
125 PZ  0.11
129 PZ  0.12
c
c  Dividing planes to vary shield opening
140 P  N  1  0  0.0001
150 P  N -1  0 -0.0001
c  change N accordingly
c  170, N=11.43 (170.00deg)
c  150, N=03.73 (149.98deg)
c  120, N=01.73 (119.94deg)
c   90, N=01.00
c   60, N=0.577 (59.970deg)
c   30, N=0.268 (30.005deg)
c   10, N=0.087 (9.9444deg)
c
c  Sphere of about 1m^3
400 SO  133.5
c

c  ---DATA CARDS---
c  Mesh Tally
*FMESH04:p  Geom = cyl  Origin = 0 0 -0.5
         AXS 0 0 1         VEC 1 0 0
         IMESH = 1 10       IINTS = 1 9
         JMESH = 1         JINTS = 1
         KMESH = 1         KINTS = 360
         OUT = col
#   DE04            DF04
    0.0010          4065
    0.0015          1372
    0.0020          615.2
    0.0030          191.7
    0.0040          81.91
    0.0050          41.88
    0.0060          24.05
    0.0080          9.915
    0.0100          4.944
    0.0150          1.374
    0.0200          0.5503
    0.0300          0.1557
```

```
   0.0400          0.06947
   0.0500          0.04223
   0.0600          0.03190
   0.0800          0.02597
   0.1000          0.02546
   0.1500          0.02764
   0.2000          0.02967
   0.3000          0.03192
   0.4000          0.03279
   0.5000          0.03299
   0.6000          0.03284
   0.8000          0.03206
   1.0000          0.03103
   1.2500          0.02965
   1.5000          0.02833
FM04  2E10
mode p
c
c Source Definitions
sdef   par = 2 pos = d1 rad = d2 axs = 0 0 1 ext = d3 erg = d4
si1    L  0 0 0
sp1    1.0000
si2    0.000  0.04
sp2    -21  1
si3    -.11 .11
sp3    0    1
[[[ENTER GAMMAS AND X-RAY ENERGIES AND FREQUENCIES HERE]]]
c
c  Materials
m1 1000.04p   0.6667  8000.04p  0.3333  $ water
[[[ENTER MATEIRAL CARD HERE]]]
m4 79000.04p -1.0000              $ Gold
c
c  Specifications
cut:p  1j  0.001
cut:e  1j  0.020
Phys:p  1  0  0  0  1
nps 50000000
```